

Video Article

Quantitative Micro-CT Analysis of Aortopathy in a Mouse Model of β -aminopropionitrile-induced Aortic Aneurysm and Dissection

Brittany O. Aicher¹, Subhradip Mukhopadhyay¹, Xin Lu², Selen C. Muratoglu¹, Dudley K. Strickland¹, Areck A. Ucuzian^{1,3}

¹Center for Vascular and Inflammatory Diseases, University of Maryland School of Medicine

²Department of Diagnostic Radiology and Nuclear Medicine, University of Maryland School of Medicine

³Division of Vascular Surgery, University of Maryland School of Medicine

Correspondence to: Brittany O. Aicher at baicher@som.umaryland.edu

URL: <https://www.jove.com/video/57589>

DOI: [doi:10.3791/57589](https://doi.org/10.3791/57589)

Keywords: Medicine, Issue 137, Aortic aneurysm, aortic dissection, animal models of human disease, β -aminopropionitrile, *in vivo* imaging, micro-computerized tomography

Date Published: 7/16/2018

Citation: Aicher, B.O., Mukhopadhyay, S., Lu, X., Muratoglu, S.C., Strickland, D.K., Ucuzian, A.A. Quantitative Micro-CT Analysis of Aortopathy in a Mouse Model of β -aminopropionitrile-induced Aortic Aneurysm and Dissection. *J. Vis. Exp.* (137), e57589, doi:10.3791/57589 (2018).

Abstract

Aortic aneurysm and dissection is associated with significant morbidity and mortality in the population and can be highly lethal. While animal models of aortic disease exist, *in vivo* imaging of the vasculature has been limited. In recent years, micro-computerized tomography (micro-CT) has emerged as a preferred modality for imaging both large and small vessels both *in vivo* and *ex vivo*. In conjunction with a method of vascular casting, we have successfully used micro-CT to characterize the frequency and distribution of aortic pathology in β -aminopropionitrile-treated C57/Bl6 mice. Technical limitations of this method include variations in the quality of the perfusion introduced by poor animal preparation, the application of proper methodologies for vessel size quantification, and the non-survivability of this procedure. This article details a methodology for the intravascular perfusion of a lead-based radiopaque silicone rubber for the quantitative characterization of aortopathy in a mouse model of aneurysm and dissection. In addition to visualizing aortic pathology, this method may be used for examining other vascular beds *in vivo* or vascular beds removed post-mortem.

Video Link

The video component of this article can be found at <https://www.jove.com/video/57589/>

Introduction

The incidence of aortic dissection is 3 cases per 100,000 per year¹. Aortic dissection and aneurysmal diseases account for over 10,000 deaths in the United States each year, accounting for 1 - 2% of all deaths in Western countries². Aortic dissection is initiated by a tear in the intimal layer of the vessel with the propagation of blood through the layers of the aortic wall under physiologic pressures. Elevated patient pulse pressures are associated with an increased incidence of dissection and complications. Increased wall shear stress is associated with the aortic wall expansion leading to an aneurysm formation^{3,4}. Consequences of aortic dissection include the occlusion of blood flow to distant organs including the brain, kidneys, bowels, and limbs, the formation of chronic aneurysms, rupture, or death^{5,6,7}.

At present, the biochemical and cellular processes involved in the initiation and progression of aortic aneurysms and dissections are still poorly understood. Reproducible animal models of aortic aneurysm and dissection are key to understanding their pathophysiology. β -aminopropionitrile (BAPN) is a lysyl oxidase inhibitor, which prevents the cross-linking of elastin and collagen and has been shown to significantly alter the structure of the vessel wall extracellular matrix and its biomechanical integrity^{6,8}. Rodents treated with BAPN have been utilized as a common animal model of aortic aneurysm and dissection^{9,10}.

Vascular imaging modalities are instrumental in identifying vascular pathology, confirming vessel patency, and evaluating organ perfusion. Recently, micro-computed tomography (micro-CT) has been utilized to study the vasculature of mice and similarly sized animals. Unlike bone, the axial imaging of blood vessels by computed tomography is limited, as intraluminal blood is inherently relatively radiolucent. When combined with intravascular contrast agents, however, micro-CT enables detailed three-dimensional reconstructions of animal vasculatures for the study of macro-anatomic vascular pathology¹¹.

The selected contrast agent (see the **Table of Materials**) is a radiopaque silicone rubber that contains lead chromate and lead sulfate. Upon perfusion in the presence of a catalyst, it quickly hardens to form a cast of the vasculature with minimal alterations in the macro-anatomic architecture of the vessels, making the vasculature highly radiopaque in contrast to the background tissues when examined radiographically. This contrast agent is advantageous because it is easy to handle and avoids the tissue degradation and vessel loss due to breakage often associated with vascular cast corrosion. As it cures with minimal shrinkage¹², vessels cleared of blood remain patent and allow for an accurate assessment of the animal macro-vasculature in non-survival experiments. Previous work has successfully used radiopaque silicone rubber-contrast in a variety of animal studies. Specifically, applicability in visualizing the coronary, glomerular, placental, and cerebral circulations^{11,12,13,14,15} has been

shown. In this paper, we detail the methodology of open left-ventricular puncture for the intravascular perfusion of lead-based radiopaque silicone rubber to quantitatively characterize BAPN-induced aortic pathology in a mouse model by micro-CT.

Protocol

The protocols for animal handling were approved by the Institutional Animal Care and Use Committee of the University of Maryland, Baltimore (animal protocol number 0116024) and conducted according to AAALAC International standards.

1. Preparation of Reagents

1. Heparin

1. Dilute 250 μ L of 1000 U/mL heparin sulfate in 50 mL of phosphate buffered saline to make a final concentration of 5 U/mL.
2. Warm the heparinized (5 U/mL) phosphate buffered saline, which will replace the blood in the vasculature in a water bath set to 37 °C.
3. Prepare the pressure-controlled pump by connecting the required tubing and 2 empty 10-mL syringes, 1 for the heparinized-saline buffer and 1 for the contrast agent.
4. Fill the tubing with the warm heparinized phosphate buffered saline and remove the air bubbles from the tubing of the pressure pump.

2. Contrast agent

NOTE: Please refer to the **Table of Materials** for the contrast agent kit constituents.

1. Mix a pigmented compound with a diluent to achieve a 1:6 dye to diluent ratio.
2. Immediately prior to use (step 2.3.12), add 200 μ L of a curing agent to each 5-mL aliquot of the diluted pigmented compound and mix them well (4% by volume).

NOTE: The manufacturer reported the working time is 40 min. As the silicone-rubber contrast agent begins to polymerize 20 min after the addition of the curing agent, it is important to prepare the solution immediately prior to its infusion.

3. BAPN drinking water

1. Dissolve β -aminopropionitrile (BAPN) in drinking water to create a final concentration of 3 g/L (adapted from protocols previously described in the literature)^{9,16,17}.
2. Administer the BAPN-containing drinking water to a group of mice once they are 4 weeks of age until the time of perfusion for micro-CT.

2. Surgical Procedure

1. Animal preparation

1. Wean the mice at 3 weeks of age, maintain them on a 12 h light/12 h dark cycle, and feed them standard rodent chow. For the BAPN-treated group, administer freshly prepared BAPN drinking water for 16 - 26 weeks *ad libitum*. Provide the control animals with standard drinking water *ad libitum*.

2. Anesthetic technique

NOTE: 24 h prior to the CT analysis, the following procedure is performed. Surgical procedures are enacted to prepare the specimen for a postmortem intracardiac perfusion.

1. Induce an anesthesia via an induction tank with 100% O₂ and 3% isoflurane delivered via a precision vaporizer. After the anesthesia induction, discontinue the isoflurane and flush the chamber with O₂. Maintain the anesthesia with 2 - 2.5% isoflurane and 1 L/min of O₂ via a nose cone.
2. Attach both the induction chamber and the facemask to a charcoal scavenger for waste gas adsorption to protect personnel. Ensure an adequate anesthetic plane by demonstrating that there is no response to noxious stimuli (toe pinch).
3. Prepare an operative field consisting of a surgical tray and the necessary surgical instruments.
4. Transfer the animal to the surgical field and position it in dorsal recumbency.

3. Operative technique

1. Using scissors, make a midline incision through the skin and soft tissue from midway between the pubic symphysis to the sternal notch, extending through the skin and soft tissue overlying the sternum.
2. Using scissors, create a hole in the diaphragm at the xiphoid process to enter the thoracic cavity.
3. Use scissors to dissect the diaphragm of the ventral chest wall, bilaterally.
4. Cut through the costal cartilages to separate the ribs from the sternum at the right sternal border.
5. Apply a fine hemostatic clamp to the tip of the sternum (near the xiphoid process) and move the hemostat cranially so that it is positioned over the head of the mouse. This will retract the thymus and sternum away from the heart, exposing the heart and great vessels for further manipulation.
6. Sharply dissect any attachments between the heart and the chest wall.
7. Connect the 27-gauge IV catheter needle to a syringe pre-loaded with 10 mL of heparinized phosphate buffered saline (5 U/mL) and fill all tubing with the buffer in order to remove the air bubbles from the tubes of the pressure pump.
8. Use care while preparing the fluid as bubbles in the fluid line may impede the filling of smaller vessels. Limit the number of vessels that are damaged during the animal preparation, as this will cause the contrast agent to leak out of the severed vessels, changing the volume required for a complete filling and introducing artifacts to the final imaging.
9. Puncture the left ventricle with a 27-gauge needle that is stabilized with a right-angle clamp. Immediately incise the right ventricle or the inferior vena cava to drain the heparin solution and blood.

NOTE: Heparin is used as an anticoagulant to prevent the blood from clotting in the vessels after the animal's death.

10. Perfuse the animal at a constant rate of 2 mL/minute using a single syringe pump. Note the visible blanching of the organs. Continue the perfusion until the perfusate draining from the venous circulation is free of blood (about 5 - 6 mL). Stop the pump.
11. Disconnect the IV catheter tubing from the 10-mL syringe, taking care not to disrupt the needle's position in the left ventricle.
12. Immediately after the complete exsanguination, separate the contrast agent solution into 5-mL aliquots and add the curing agent at this time (see step 1.2). Mix them well. Draw up 5 mL of the contrast agent mix into a 10-mL syringe and perfuse the animal with it.
13. For a complete filling of the vessels (arteries and veins), continue the infusion past the point when it can be seen exiting the venous solution. Look for signs of a successful perfusion including the visualization of a casting agent in the coronary arteries, pulmonary arteries, intestine, and liver vasculature.
14. The contrast agent will cure after approximately 20 min at room temperature. Upon curing, harvest the individual organs, as needed, and fix them in 10% neutral buffered formalin. Fix whole carcasses if the samples are not used for micro-CT scanning the following day. If the carcasses will be used the subsequent day, position them on a metal tray and place them in a refrigerator at 4 °C to cure overnight.

3. Micro-CT Scanning and Parameters

NOTE: The specific image acquisition parameters will be dependent upon the machine in use.

1. Acquire X-ray computed tomography images of each mouse the day following the perfusion using a micro-CT scanner using an X-ray tube voltage of 55 kVp, a current of 150 μ A, a system magnification factor of 2.19, and a CCD camera pixel binning factor of 2. This yields an effective pixel size of 29 μ m.
 1. Lay the mouse carcass supine on the micro-CT scanner table and obtain a scout X-ray scan.
 2. Focus the detector field of view of 57.4 mm (axial) x 37.1 mm (transaxial) on the torso to image the full length of the aorta.
 3. Acquire 180 image projections with a rotation increment of 2 degrees and a time per projection of 2800 ms.
2. Reconstruct the images using a modified Feldkamp algorithm; the reconstructed voxel size is 29 x 29 x 29 μ m³ (slice thickness = 29 μ m) using the **Multimodal 3D Visualization** plug-in for the software used here.

4. Post-processing and Rendering

1. Convert the CT data to a DICOM format using the appropriate software.
2. Analyze the images to identify whether an aneurysm was present. Measure the minor axis diameter at the widest point of the aortic arch, descending thoracic aorta, and abdominal aorta as previously described¹⁸ (**Figure 1**).
NOTE: In our study, images were analyzed by two independent observers (one blinded) utilizing a DICOM viewer to identify whether an aneurysm was present. The minor axis diameter was measured at the widest point of the aortic arch, descending thoracic aorta, and abdominal aorta as previously described¹⁹ (**Figure 1**). Mean non-aneurysmal arterial segments of BAPN-untreated mice established normal vessel diameters serving as the age-matched control values.
3. Aneurysms are defined as a localized or diffuse dilation of the aortic segments to diameters greater than 50% of the reference diameter. Locate these based on the above measurements.

Representative Results

In order to evaluate this protocol, 20 male adult mice, of mixed background as previously described¹⁹ and of 20 - 30 weeks of age, with or without BAPN treatment, were perfused with a lead-based radiopaque silicone rubber (see the **Table of Materials**) using the protocol detailed above. They underwent micro-CT scanning on the following day (**Figure 1** and **Figure 2**). There were no significant differences in the ages of the mice among any of the compared groups.

Minor axis diameters were then quantified in these mice. The mean diameter of the ascending aorta in the BAPN-treated mice was significantly larger than that of the untreated age-matched controls (1.43 ± 0.56 mm vs. 0.93 ± 0.11 mm; $p = 0.023$, unpaired Students *t*-test). The inhibition of lysyl oxidase with BAPN did not have a significant effect on the mean descending thoracic or abdominal aortic diameters compared to the age-matched controls ($p > 0.082$, unpaired Students *t*-test, **Figure 3**).

An aneurysm was defined as being 1.5x the mean diameter of the untreated group. There was a significant increase in the number of mice with aneurysms in the BAPN-treated compared with the BAPN-untreated controls (50% of the BAPN-treated mice vs. 0% of the untreated mice; $P = 0.042$) by Fisher's exact test. Aneurysms in the BAPN-treated mice were identified exclusively in the aorta, with the majority identified in the thoracic aorta (8 out of 10 aneurysms identified). 4 mice developed more than 1 aneurysm with the BAPN-treatment (**Table 1**).

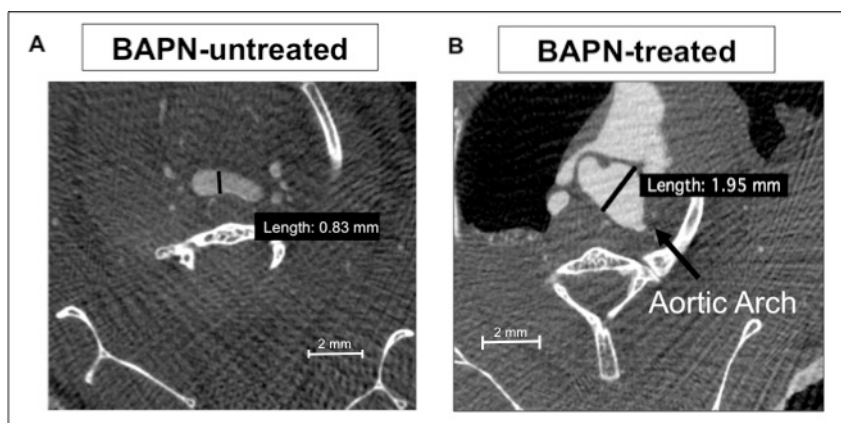


Figure 1: Representative cross-sectional micro-CT images. **A.** This is a cross-sectional imaging of the BAPN-untreated mice. **B.** This is a cross-sectional imaging of the BAPN-treated mice. The minor axis diameter measurements are made at the level of the aortic arch.

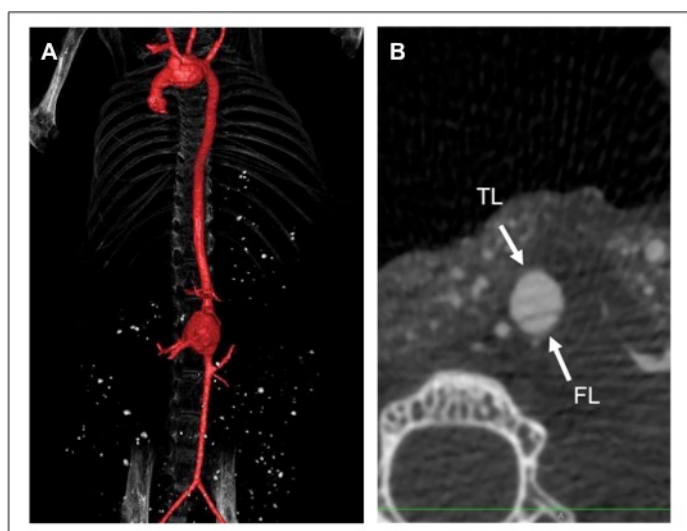


Figure 2: Three-dimensional reconstruction of mouse aortic aneurysm and dissection identified by micro-CT. **A.** This is a representative 3-D reconstruction of a BAPN-treated mouse with a sacular abdominal aortic aneurysm and an aortic arch aneurysm. **B.** This panel shows a representative descending thoracic aortic dissection in a BAPN-treated mouse. The true and false lumen are separated by the intimal flap. The true lumen (TL) is the normal passageway of blood and the false lumen (FL) is the newly created passageway.

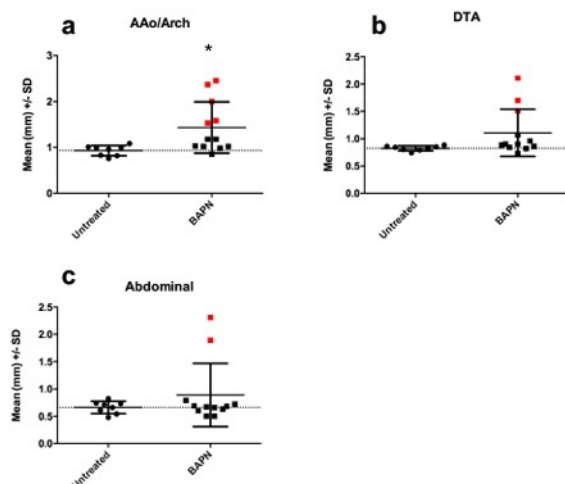


Figure 3: Effect of BAPN treatment on aortic diameters. These panels show the mean minor axis vessel diameters measured by micro-CT in BAPN-untreated and BAPN-treated male mice. Those mice determined to have an aneurysm are highlighted in red. The mean of the untreated group is represented as a dotted line in each panel. **a.** This is the ascending aorta/arch (AAo/Arch); 0.93 ± 0.11 vs. 1.43 ± 0.56 mm; $p = 0.023$. **b.** This is the descending thoracic aorta (DTA); 0.82 ± 0.04 vs. 1.11 ± 0.43 mm; $p = 0.0817$. **c.** This is the abdominal aorta; 0.66 ± 0.11 vs. 0.89 ± 0.58 mm; $p = 0.296$. All data are presented as mean \pm standard deviation. [Please click here to view a larger version of this figure.](#)

	No BAPN (n = 8)	BAPN (n = 12)
Total Animals with Aneurysm	0	6 *
Total Number of Aneurysms	0	10
AAO/ARCH	0	5
DTA	0	3
ABD AORTA	0	2

Table 1. Anatomic distribution of identified aneurysms in male mice with and without BAPN treatment. This table shows the incidence of aneurysms as identified by micro-CT (n = 20). AAO = ascending aorta; DTA = descending thoracic aorta; ABD AORTA = abdominal aorta. * $p < 0.05$.

Discussion

Micro-CT imaging can be used to provide highly detailed and three-dimensional reconstructions of vascular pathology in animal models. Through the use of intravascular contrast-enhanced media, non-enhanced soft tissues, such as the lumen of a blood vessel, can be differentiated from those that are enhancing. While laser Doppler, microangiography, magnetic resonance angiography, histology with confocal, or two-photon microscopy may be used to assess vascular beds, they typically focus on a limited area of study and/or are limited to two-dimensional assessments. Micro-CT provides a cost-effective means of obtaining detailed imaging of vascular structures, which can aid in gaining an understanding of the underlying angiogenesis and vascular biology. Additional methods of imaging small animals include *in vivo* micro-CT and digital subtraction angiography. Similar to the technique described here, *in vivo* micro-CT relies upon an exogenous contrast agent to increase the resolution. Fenestra VC and Isovue-370 are 2 such blood-pool contrast agents that are available for micro-CT. Fenestra VC has been used and is reported to have a maximum mean enhancement of ~620 Hounsfield Units in the aorta 20 min following injection²⁰. Other nanoparticle-based contrast agents have also shown potential in both CT and MRI. Left ventricular catheterization without opening the chest is another method of whole mouse perfusion for microimaging that has been described²¹. Ultrasound imaging for the longitudinal measurements of a vessel diameter is a final method that can be used in survival studies.

During this procedure, adequate perfusion requires a high degree of attention to detail. It is important for the vasculature to be completely exsanguinated prior to the perfusion with a contrast agent. If the liver does not blanch and remains its dark red color, additional flushing with a heparinized saline solution may be needed prior to the perfusion with a contrast. Incomplete exsanguination of the vasculature may affect the final image quality, appearing as filling defects in the vasculature or as artifactual distal vascular occlusions. Further, the insertion of the needle into the left ventricle is a delicate procedure that can tear the ventricular wall or cut through into the right ventricle. If the needle is inserted into the right ventricle, the lungs will be perfused quickly and will turn yellow early during the perfusion, leading to an incomplete vascular perfusion. A vessel rupture is a final complication that leads to an incomplete perfusion. The chance of a vessel rupture can be minimized by ensuring adequate drainage from the venous circulation prior to initiating the perfusion via the arterial tree. Retrograde injection is an alternative method to perfusing a vascular bed, which has previously been described to image the coronary vasculature¹¹. We chose an antegrade method of perfusion as it more accurately represents physiologic blood flow in the thoracic and abdominal aorta. The quality of the image obtained with micro-CT does limit the ability to assess the aorta for intramural thrombus or hematoma. However, the soft tissue can be visualized quite well depending on how the CT protocol is formulated. For our studies, we noticed segments of the aorta with filling defects presumably due to stenoses from intraluminal thrombus. The technique as described is best for assessing the intravascular space.

In summary, this protocol provides a safe technique for the high-resolution examination of the vasculature of a murine model of aortic aneurysm and dissection. Quantitative analyses can be easily achieved using micro-CT images, which are able to provide a precise cast of the vasculature. For the purposes of the experiments illustrated in this publication, we chose to measure the largest aortic diameter to mimic the measurement of aortic aneurysms in clinical practice. A combination of anatomic landmarks and slice location distances can be utilized to measure specific segments of the aorta if appropriate. It is also shown that the perfused animal vasculature can be imaged and digitally separated from the skeletal background to the desired amount to create a three-dimensional representation of the major blood vessels and its smaller distal branches. This protocol preserves the vascular tissues of interest, which can be embedded in paraffin and used for histological sectioning for further examination.

Micro-CT is a promising imaging modality for the study of vascular biology. With its high spatial resolution, it offers an opportunity to evaluate the structure, organization, and pathology of blood vessels. The procedure described in this manuscript requires multiple skills and techniques including animal handling and preparation, image acquisition, and quantification of the results. This article has successfully demonstrated one application of vascular perfusion to identify aortopathies in mice. Further studies are needed to assess its applicability in other animal models and disease processes.

Disclosures

The authors have nothing to disclose.

Acknowledgements

We would like to thank Mark Smith for his assistance with radiographic imaging. This work is supported by the NIH T32 Grant for Interdisciplinary Research in Cardiovascular Disease (BOA), the American Heart Association (SMC), and the NIH R35 Grant (DKS).

References

- Meszaros, I., *et al.* Epidemiology and clinicopathology of aortic dissection. *CHEST*. **117** (5), 1271-1278 (2000).
- Kochanek, K.D., *et al.* Deaths: final data for 2009. *National Vital Statistics Reports*. **60** (3), 1-116 (2011).
- Li, J.S., Li, H.Y., Wang, L., Zhang, L., Jing, Z.P. Comparison of beta-aminopropionitrile-induced aortic dissection model in rats by different administration and dosage. *Vascular*. **21** (5), 287-292 (2013).
- Huffman, M.D., Curci, J.A., Moore, G., Kerns, D.B., Starcher, B.C., Thompson, R.W. Functional importance of connective tissue repair during the development of experimental abdominal aortic aneurysms. *Surgery*. **128** (3), 429-438 (2000).
- Wu, D., Shen, Y.H., Russel, L., Cosell, J.S., LeMaire, S.A. Molecular mechanisms of thoracic aortic dissection. *Journal of Surgical Research*. **184** (2), 907-924 (2013).
- Bruehl, A., Ortoft, G., Oxlund, H. Inhibition of cross-links in collagen is associated with reduced stiffness of the aorta in young rats. *Atherosclerosis*. **140** (1), 135-145 (1998).
- Martinez-Revelles, S., *et al.* Lysyl oxidase induces vascular oxidative stress and contributes to arterial stiffness and abnormal elastin structure in hypertension: Role of p38MAPK. *Antioxidants & Redox Signaling*. **27** (7), 379-397 (2017).
- Kumar, D., Trent, M.B., Boor, P.J. Allylamine and beta-aminopropionitrile induced aortic medial necrosis: Mechanisms of synergism. *Toxicology*. **125** (2-3), 107-115 (1998).
- Ren, W., *et al.* B-Aminopropionitrile monofumarate induces thoracic aortic dissection in C57BL/6 mice. *Scientific Reports*. **6**, 28149 (2016).
- Kanematsu, Y., *et al.* Pharmacologically-induced thoracic and abdominal aortic aneurysms in mice. *Hypertension*. **55** (5), 1267-1274 (2010).
- Weyers, J.J., Carlson, D.D., Murry, C.E., Schwartz, S.M., Mahoney Jr., W.M. Retrograde Perfusion and Filling of Mouse Coronary Vasculature as Preparation for Micro Computed Tomography Imaging. *J Vis Exp*. (60) 1-8 (2012).
- Cortell, S. Silicone rubber for renal tubular injection. *Journal of Applied Physics*. **26** (1), 158-159 (1969).
- Bentley, M.D., Ortiz, M.C., Ritman, E.L., Romero, J.C. The use of microcomputed tomography to study microvasculature in small rodents. *American Journal of Physiology - Regulatory, Integrative and Comparative Physiology*. **282** (5), R1267-R1279 (2002).
- Marxen, M., *et al.* MicroCT scanner performance and considerations for vascular specimen imaging. *Medical Physics*. **31** (2), 305-313 (2004).
- Yang, J., Yu, L.X., Rennie, M.Y., Sled, J.G., Henkelman, R.M. Comparative structural and hemodynamic analysis of vascular trees. *American Journal of Physiology - Heart and Circulatory Physiology*. **298** (4), H1249-H1259 (2010).
- Jia, L.X., *et al.* Mechanical stretch-induced endoplasmic reticulum stress, apoptosis, and inflammation contribute to thoracic aortic aneurysm and dissection. *The Journal of Pathology*. **236** (3), 373-383 (2015).
- Kurihara, T., *et al.* Neutrophil-derived matrix metalloproteinase 9 triggers acute aortic dissection. *Circulation*. **126** (25), 3070-3080 (2012).
- Dillavou, E.D., Buck, D.G., Muluk, S.C., Makaroun, M.S. Two-dimensional versus three-dimensional CT scan for aortic measurement. *Journal of Endovascular Therapy*. **10** (3), 531-538 (2003).
- Muratoglu, S.C., *et al.* LRP1 protects the vasculature by regulating levels of connective tissue growth factor and HtrA1. *Arteriosclerosis, Thrombosis, and Vascular Biology*. **33**, 2137-2146 (2013).
- Badea, C.T., Dragova, M., Holdsworth, D.W., Johnson, G.A. In vivo small animal imaging using micro-CT and digital subtraction angiography. *Phys Med Biol*. **53**(19):R319-50 (2008).
- Zhou, Y.Q., *et al.* Ultrasound-guided left-ventricular catheterization: A novel method of whole mouse perfusion for microimaging. *Laboratory Investigation*. **84**, 385-389 (2004).